Front. Earth Sci. 2023, 17(1): 158−169
https://doi.org/10.1007/s11707-022-1038-6

RESEARCH ARTICLE

Accumulation model and geochemistry characteristics of oil occurring from Jurassic coal measures in the Huangling mining area of the Ordos Basin, China

Yuan BAO (✉)[1,2], Yiliang HU[1], Wenbo WANG[1], Chen GUO[1], Guochang WANG[3]

1 College of Geology and Environment, Xi'an University of Science and Technology, Xi'an 710054, China
2 Key Laboratory of Coal Resources Exploration and Comprehensive Utilization, Xi'an 710021, China
3 Engineering Department, Saint Francis University, Loretto, PA 15940, USA

Abstract The Ordos Basin is an important intracontinental sedimentary basin in China, containing a significant amount of coal, oil, and natural gas. This study analyzed the sedimentary environment, sedimentary facies, parent material type, maturity, and carbon isotopic composition of the coal-bearing organic matter using gas chromatography–mass spectrometry (GC–MS) and stable isotope ratio mass spectrometry. The source of oil occurring in the No. 2 coal seam of the Jurassic Yan'an Formation (An-1 oil) and its accumulation model were also investigated. The results show that the relative abundances of C_{27}, C_{28}, and C_{29} steranes in the An-1 oil are 43.8%, 33.0%, and 23.2%, respectively. The tricyclic terpanes, C_{29}20S/(20S + 20R), and $C_{29}\beta\beta/(\beta\beta+\alpha\alpha)$ contents of the An-1 oil are 31.4%−34.8%, 0.85 and 0.81, respectively. Pr/n-C_{17}, Ph/n-C_{18}, and Pr/Ph values are 0.34, 0.42, and 0.87, respectively. Biomarker parameters indicate that the An-1 oil mainly comes from the plankton source rock deposited in the freshwater lake facies and a reducing environment, which has evolved to maturity. The correlation of oil-oil indicates that the An-1 oil is homologous to the Chang-7 oil (Chang-7 member of the Triassic Yanchang Formation). The correlation of oil-source rock presents that the An-1 oil is generated from the Yanchang Formation (Chang-6 and Chang-7 source rocks) and occurred in the coal seam during the stage of stratum uplift since the Early of Late Cretaceous. The distribution characteristics of $\delta^{13}C_{\text{group components}}$ in the An-1 oil and Chang-7 oil also reveal the fractionation phenomenon during the migration of crude oil.

Keywords coal measures, oil source, biomarker compounds, carbon isotope, Ordos Basin

Received March 22, 2022; accepted September 8, 2022

E-mail: y.bao@foxmail.com

1 Introduction

There are abundant industrial raw materials with economic values in coal measures, such as aluminum, iron, lithium, germanium, gallium, kaolin, clay ore, graphite, coal, oil, and methane (Ward, 2002; Li et al., 2019a, 2022). Among them, organic carbons (coal, oil, and methane) are the lifeblood of national economic development and the cornerstone of national strategy development. With the increase of environmental protection by international community and the propose of achieving a carbon peak by 2030 and carbon neutral by 2060 in China, the utilization pattern of coal has gradually changed from the traditional energy source for generating power to coal gasification, and liquefaction integrated with CO_2 capture and storage (Jiang and Bhattacharyya, 2016; Huang et al., 2017; Su et al., 2022). Methane is relatively clean fossil energy. When natural gas occurs in the coal seam, shale, and tight sandstone, it is called unconventional natural gas (Li et al., 2019a). Therefore, it is of great significance to study unconventional natural gas, especially their resource potential and occurrence state in the coal measure.

In the coal measure, there exist two important hydrocarbon source rocks, including coal and organic shale. Both of them have a good potential for oil and gas generation (Hunt, 1991). Therefore, the coal seam is often co-existed with oil and gas. The origin of the coal seam gas (or coalbed methane) can be identified by the gas composition, the carbon isotope composition of methane and carbon dioxide, and the hydrogen isotope composition of methane (Whiticar, 1996; Kotarba, 2012; Bao et al., 2020, 2021a). Oil source identification mainly relies on biomarker compounds, isotopes, light hydrocarbons and other indicators. Biomarker compounds contain a large amount of fingerprint information, which can provide information on crude oil deposition environment, sedimentary facies, parent material type and maturity (Ji et al., 2016; Xiao et al., 2018; Wang et al., 2020; Abdullah et al., 2021). However, biomarker compounds with low content are easily affected by the biodegradation and thermometamorphism resulting in it unable to accurately operation. Isotopes and light hydrocarbons can complement the information provided by biomarker compounds to a certain extent. Therefore, the combination of these three indicators can significantly improve the accuracy and authenticity of oil source comparison.

This study aims to explore the geochemical characteristics and sources of the Jurassic coal-bearing oil in the Huangling mining area on the southern margin of the Ordos Basin. We collected five samples, including two coals and one crude oil from the Jurassic Yan'an Formation, as well as two crude oils from the Triassic Yanchang Formation. The gas chromatography–mass spectrometry (GC-MS) and stable isotope ratio mass spectrometry were employed to characterize the biomarker compounds and carbon isotopes of crude oil and source rock, respectively. The characteristics of *n*-alkanes, acyclic isoprenoids, tricyclic terpenes, steranes, and carbon isotopes of total hydrocarbon and different group components were analyzed. The oil source and accumulation pattern of crude oil occurring in the coal measures were discussed based on various biomarker indicators. This research is of great significance for identifying the sources of oil in the study area and improving the safety of coal production.

2 Geological setting

The Ordos Basin is the second-largest petroliferous basin in China. The main internal structure is dominated by uplifts and depressions, forming many wide and gentle folds (Li et al., 2017a, 2019b). The external structure deformation was strong, and folds and faults were developed (Deng et al., 2005). The Meso-Cenozoic multicycle tectonic evolution in the basin eventually formed six structural units of the Yimeng uplift, western fold-thrust belt, Tianhuan depression, northern Shaanxi slope, Jinxi flexural fold zone, and Weibei uplift (Fig. 1(a)) (Huang et al., 2015). The oil within the basin is mainly found in the Mesozoic Triassic Yanchang Formation, Jurassic Yan'an Formation, and Zhiluo Formation (Zhao et al., 2014). Triassic reservoirs were deposited within the inland lacustrine delta, mainly located in the east and south of the basin (Li et al., 2017b); Jurassic reservoirs were mainly in river-dominant delta (Liu et al., 2020).

The Huangling mining area is located on the southern

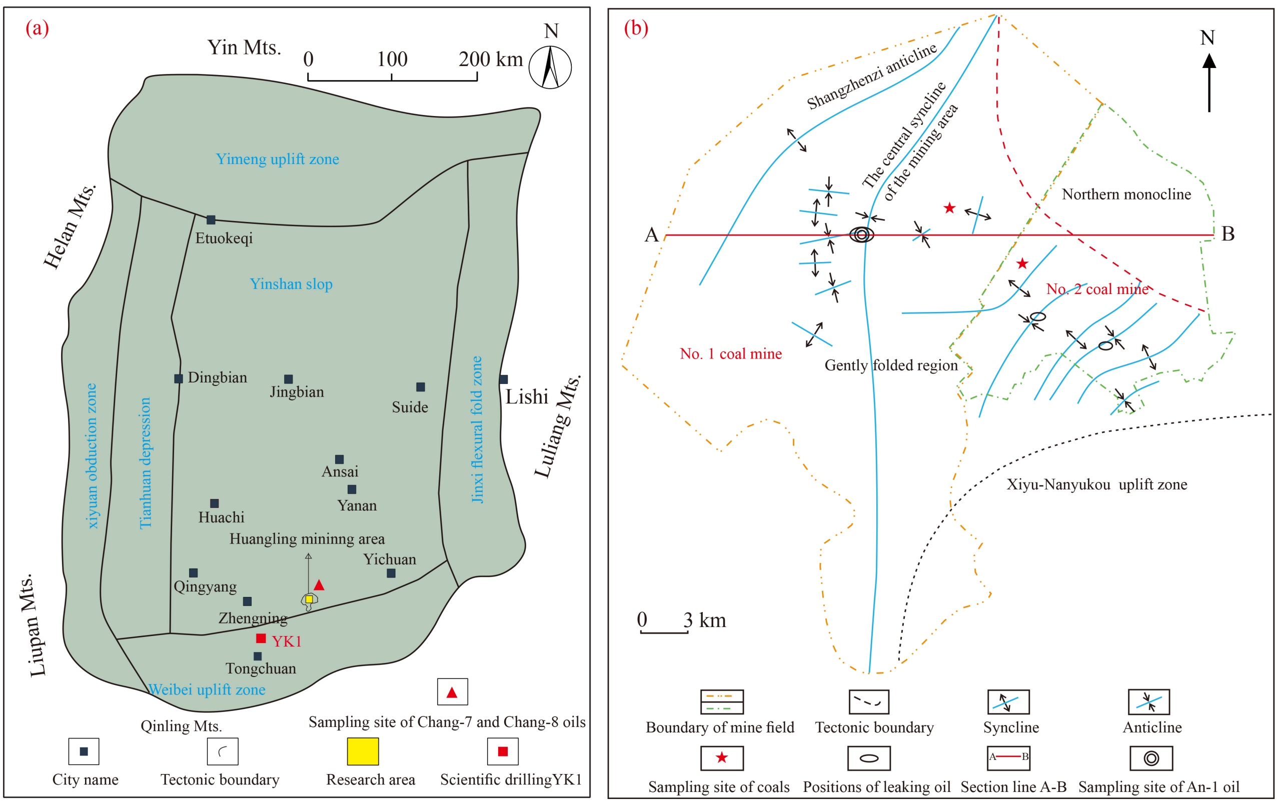

Fig. 1 Sampling location and structural outline of the study area: (a) the Ordos Basin; (b) the Huangling mining area (modified from Bao et al., 2021b).

margin of the Ordos Basin. The areas of mines No. 1 and No. 2 are 209.93 km^3 and 351.94 km^3, respectively. The primary mineable coal seam is the No. 2 coal seam of the Yan'an Formation. The thickness of the coal seam is 0.05−6.75 m, with an average of 3.12 m. There are nearly 150 oil- and gas- bearing holes in this mining area, of which 5 drilling holes showed oil and gas ejection or escape (Chen, 2018), which are typical coal-oil-gas symbiosis mines. The coal rank is subbituminous coal, and the gas genetic type is mainly a mixture of coal-type gas and oil-type gas (Li et al., 2023). When coal was mined underground, it was found that the crude oil often gushes out from the bottom of No. 2 coal seam in the mining area. This phenomenon seriously endangers the safe production of the coal mining. In the meantime, the crude oil corrodes the machinery, and it will even burn when it leaks to the working face. Therefore, it is crucial to determine the source of crude oil in the coal seam and predict the migration path of crude oil.

3 Samples and methods

3.1 Samples collection

The basic information of coal and crude oil samples are shown in Table 1. Coal samples of HL1-5 and HL2-5 were collected from the Jurassic Yan'an Formation No. 2 coal seam in the No. 1 and No. 2 coal mines of the Huangling mining area. Crude oil of An-1 was collected from the bottom of the Jurassic No. 2 coal seam in the Huangling mining area, and crude oils of Chang-7 and Chang-8 were collected from a drilling of Triassic Yanchang Formation. To enrich the research content and ensure the accuracy of oil and source rock correlation, part of the source rock data was cited from the scientific drilling YK1 by Yang et al. (2017), which is also listed in Table 1.

3.2 Sample preparation

The two coal samples were crushed and sieved to obtain a sample size ranging from 120 to 200 mesh, then dried for 12 h under 80°C. Each dried coal sample weighed 5 g and was extracted for 72 h using *n*-hexane as a solvent with a Soxhlet extraction device. The crude oil samples (50 mg) were extracted using 30 mL *n*-hexane to precipitate asphaltenes and stand for more than 12 h. Then, a chromatography column which was filled with 3:2 silica gel to alumina ratio was used to separate the group components (saturated hydrocarbons, aromatic hydrocarbons, and nonhydrocarbons). Saturated hydrocarbons and aromatic hydrocarbons were eluted with *n*-hexane and the mixture of dichloromethane and *n*-hexane (2:1 vol%), respectively. The nonhydrocarbons were finally eluted with ethanol and then with chloroform.

3.3 Gas chromatography–mass spectrometry (GC–MS) testing

The organic compounds extracted from crude oil and coal samples were tested by GC–MS (Agilent 7890B-5977B) with a chromatographic inlet temperature of 250°C. The carrier gas was He with a gas flow rate of 3 mL/min. The chromatographic column was an elastic quartz capillary column made in the United States (DB-1MS, 60 m × 0.25 mm × 0.25 μm). The testing temperature rose from 40°C to 325°C at a rate of 4°C/min and then remained constant for 15 min. The mass spectrometry ion source was an EI source with a temperature of 230°C. Quadrupole temperature and ionization energy were set to 150°C and 70 eV, respectively.

3.4 Stable carbon isotope testing

The stable carbon isotopic compositions of total hydrocarbon of coal, crude oil, and source rock samples and different group components of three crude oils were detected and analyzed by continuous flow using a MAT253 isotope mass spectrometer combined with a FLASH HT elemental analyzer. The crude oils and its four extractable group components were weighted 2 mg and wrapped in a tin capsule for carbon isotope testing. The element analyzer used the oxidation method to

Table 1 Samples' basic information

Sample ID	Type	Formation/Systerm	Description
HL1-5 coal	Coal	Yan' an/Jurassic	Organic matter content is 98.70%, R_o = 0.67%
HL2-5 coal	Coal	Yan' an/Jurassic	Organic matter content is 93.04%, R_o = 0.71%
Chang-7 oil	Crude oil	Yanchang/Triassic	Light yellow liquid, more clear, less dense (ρ < 1 g/cm^3)
Chang-8 oil	Crude oil	Yanchang/Triassic	Yellowish-brown liquid, turbid and less dense (ρ < 1 g/cm^3)
An-1 oil	Crude oil	Yan' an/Jurassic	Dark brown liquid, cloudy, low density (ρ < 1 g/cm^3)
Chang-6 mudstone*	Source rock	Yanchang/Triassic	Gray black mudstone, thickness of formation is 40.2 m
Chang-7 shale*	Source rock	Yanchang/Triassic	Black oil shale, thickness of formation is 12.7 m
Chang-8 mudstone*	Source rock	Yanchang/Triassic	Gray black mudstone, thickness of formation is 27 m

Note: * data are cited from Yang et al. (2017).

convert the carbon in the sample into carbon dioxide. The filler of the oxidation reaction tube was chromium trioxide, reduced copper and silver-plated cobalt oxide from top to bottom. The temperature of the oxidation furnace was 940°C, and the carrier gas was helium. The carrier gas flow rate of the reaction tube was 100 mL/min, and the gas injection time was 4 s. During carbon isotopes measurement, water in the reactant was adsorbed by magnesium perchlorate. The ion source of the mass spectrometer was an EI ionization source, the ion temperature was 250°C, and the emitted electron energy was 70 eV. The standard samples used for carbon isotope detection were IAEA-600 and NBS-22.

4 Results and analysis

4.1 Biomarkers compositions

4.1.1 Normal alkanes and acyclic isoprenoids (m/z = 85)

The distribution characteristics of *n*-alkanes can effectively reflect the information of sedimentary environment, source of parent materials, maturity of organic matter (Volkman et al., 1983; Yang et al., 2017). The m/z = 85 mass chromatograms of the An-1 oil, Chang-7 oil, and Chang-8 oil all show a distribution characteristic of mono-peak model and bias to heavy molecular end. The carbon number distribution of crude oils *n*-alkanes ranges from C_9 to C_{32}, and the main peak carbon is C_{21} (Fig. 2). The *n*-alkanes distribution pattern of the extracted organic matter from HL1-5 and HL2-5 coal samples are bimodal post-peak types, and the main peak carbons of HL1-5 and HL2-5 coal samples are C_{22} and C_8, respectively. The carbon number distribution ranges from C_8 to C_{30} (Fig. 2). Therefore, three crude oils samples display similar characteristics of peak type and main peak carbon distribution but different characteristics from the coal samples.

The ratio of pristane to phytane (Pr/Ph) is an indicator of the changes of the sedimentary environment in the comparative study of oil sources (Zhang et al., 2020). The Pr/Ph values of An-1, Chang-7, and Chang-8 crude oils in the study area are 0.87, 0.97, and 1.23, respectively, and the extracted organic matter of HL1-5 and HL2-5 coals are 3.42 and 2.29, respectively (Table 2). In the source rocks of the Yanchang Formation, the Pr/Ph distribution range is 0.64−0.93 with an average of 0.75 in Chang-6 mudstone, 0.54−0.84 with an average of 0.72 in Chang-7 shale, and 1.28−1.4 with an average of 1.34 in Chang-8 mudstone (Yang et al., 2017). The Pr/Ph values of An-1 oil, Chang-7 oil, Chang-6 mudstone, and Chang-7 shale are less than 1, indicating that the organic matters' sedimentary environment of these crude oils and source rocks are formed in a reducing environment (Brooks and Smith, 1969). The Pr/n-C_{17} and Ph/n-C_{18} values of An-1 oil are 0.34 and 0.42, respectively, also implying a reducing environment. In contrast, the organic matters of the Chang-8 oil, Chang-8 mudstone, and HL1-5 and HL2-5 coals are formed in the oxidized water environment since their Pr/Ph values are larger than 1 (Zhang et al., 2020).

CPI (carbon preference index) and OPE (odd/even predominance) values often indicate the sedimentary environment and maturity of source rock (Yang et al., 2017; Fu et al., 2019). The CPI and OEP values of An-1 oil are 1.29 and 1.06, respectively. OEP value of An-1 oil ranges 1.0−1.2, closes to Chang-7 and Chang-8 oils and source rocks (Chang-6, Chang-7, and Chang-8), indicating that the An-1 oil, Chang-7 oil, Chang-8 oil and sources rocks (Chang-6, Chang-7, and Chang-8) all enter into maturity stage. Meanwhile, CPI and OEP values of coal samples (HL1-5 and HL2-5) are rather different from An-1 oil, implying that An-1 oil did not come from coal seam. In addition, according to the test by Yang et al. (2017), CPI and OEP of source rock sample are slightly greater than 1. These CPI and OEP data of oil, coal and source rocks indicate that crude oil has odd-carbon predominance and source rocks are basically in odd-even equilibrium. $\sum nC_{21}^-/\sum nC_{21}^+$ can be a good indicator of the source of parent materials (Li et al., 2020). The $\sum nC_{21}^-/\sum nC_{21}^+$ values of An-1 crude oil, Chang-7 crude oil, Chang-8 crude oil and coal organic matter (HL1-5 coal, HL2-5 coal) are 1.45, 1.44, 1.31, 1.05, and 1.27, respectively. This shows the parent materials of both An-1 oil and Chang-7 crude oil are primarily obtained from aquatic biological sources, such as plankton and algae. The distribution range of $\sum nC_{21}^-/\sum nC_{21}^+$ in Chang-6 mudstone is 1.39−2.01 with an average of 1.66, Chang-7 shale is 1.43−2.33 with an average of 1.81, and Chang-8 mudstone is 1.28−1.31 with an average of 1.3 (Yang et al., 2017), suggesting that the input ratio of terrigenous organic matter in Chang-8 mudstone is significantly higher than that in Chang-6 mudstone and Chang-7 shale during deposition.

4.1.2 Distribution characteristic of tricyclic terpenes (TT, m/z = 191)

The content distribution of tricyclic terpanes (i.e., C_{19+20} TT, C_{21}TT, C_{23}TT) is rarely affected by thermal maturity and biodegradation, thus it can be an important index for indicating the sedimentary facies of crude oils and source rocks (Xiao et al., 2018). Chromatograms of steranes and terpanes of organic matter in crude oil and coal are shown in Fig. 3(a). The tricyclic terpanes' distribution range of the An-1 oil, Chang-7 oil, and Chang-8 oil are 31.4%−34.8%, 31.7%−34.3%, and 31.4%−34.5%, respectively (Table 3). The relative abundances of tricyclic terpanes in the An-1 oil is similar to that of Chang-7 and -8 oils, suggesting that they are generated from the same sedimentary facies.

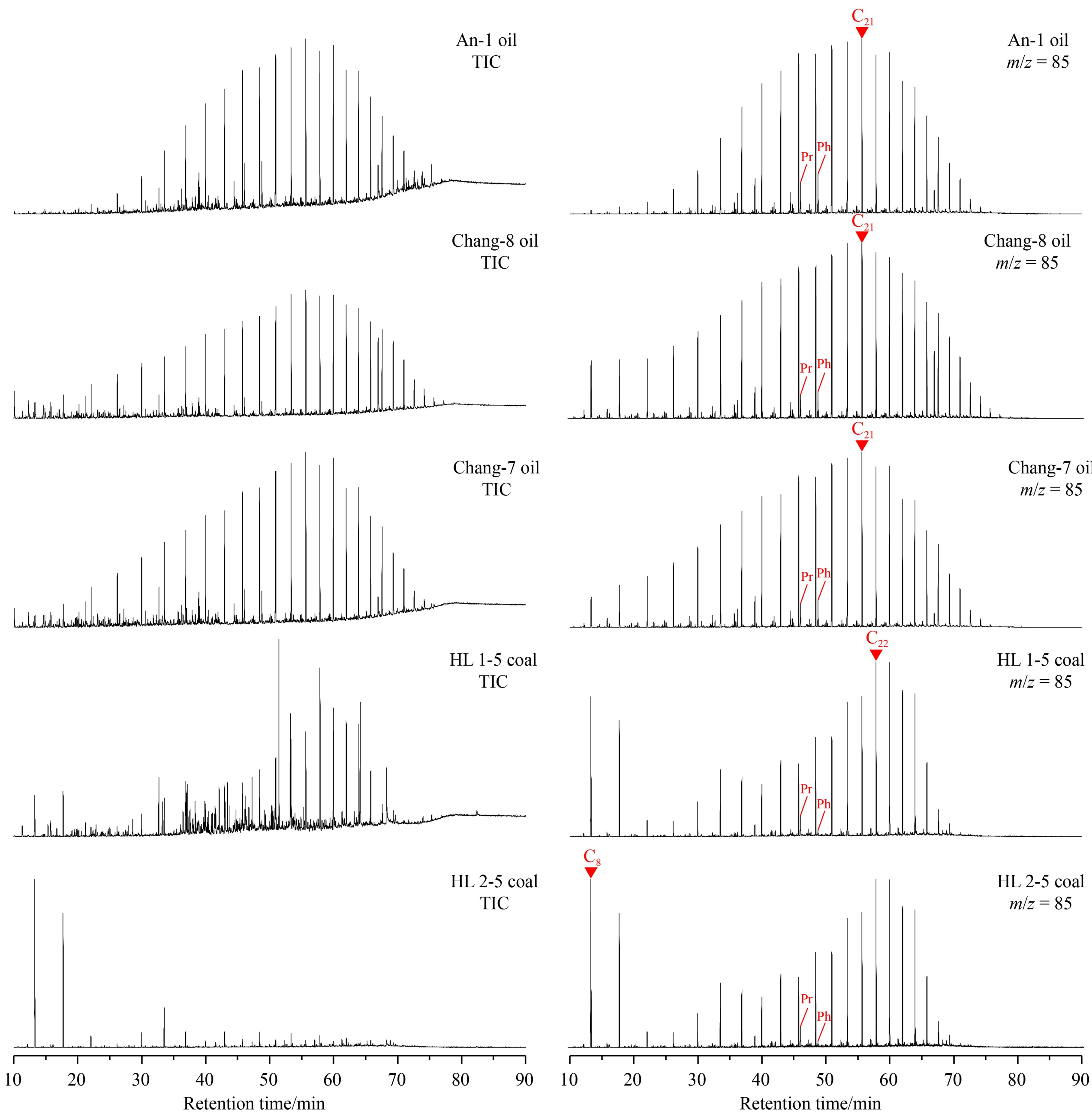

Fig. 2 Mass chromatogram of crude oils and source rocks (TIC, m/z = 85).

4.1.3 Distribution characteristic of regular steranes (m/z = 217)

The sterane isomerization parameter is the most useful and common indicator for identifying the organic matter source in crude oil among the biomarker compounds (Zhang et al., 2021). The contents of steranes in the An-1 oil, Chang-7 oil, Chang-8 oil, HL1-5 coal, and HL2-5 coal are shown in Table 3. The relative abundances of C_{27}, C_{28}, and C_{29} steranes in the Chang-6, Chang-7, and Chang-8 source rocks range from 15.0% to 40.6%, 26.5% to 34.1%, and 26.6% to 58.5%, respectively (Table 3; Yang et al., 2017). The contents of sterane C_{27}-C_{29} in the three crude oils (An-1, Chang-7, Chang-8) are 23.2%–43.8%, of which C_{27} sterane is the main component in the crude oils and C_{28} sterane is the major component in the two coal samples. The distribution characteristic and peak pattern of regular steranes are displayed in Fig. 3(b). The An-1 oil, Chang-7 oil, and Chang-8 oil are mainly characterized by the predominance of C_{27} sterane, showing an "L" distribution, while the regular sterane peak of HL1-5 and HL2-5 coal samples show predominance of C_{28} sterane and inverse "V" distribution (Fig. 3(b)). Likewise, the Chang-6 mudstone was characterized by C_{27} sterane predominance and

Table 2 Geochemical parameters of crude oil and source rocks

Sample ID	$Pr/n\text{-}C_{17}$	$Ph/n\text{-}C_{18}$	Pr/Ph	$\sum nC_{21}^{-}/\sum nC_{22}^{+}$	CPI	OEP	Main carbon
Chang-7 oil	0.48	0.5	0.97	1.45	1.11	1.09	C_{21}
Chang-8 oil	0.45	0.52	1.23	1.44	1.15	1.07	C_{21}
An-1 oil	0.34	0.42	0.87	1.31	1.29	1.06	C_{21}
HL1-5 coal	0.14	0.88	3.43	1.05	2.73	3.04	C_{22}
HL2-5 coal	0.28	0.67	2.29	1.27	3.08	0.86	C_{8}
Chang-6 mudstone*	0.47−0.78/ 0.68 (9)	0.69−1.37/ 1.03 (9)	0.64−0.93/ 0.75 (9)	1.39−2.01/ 1.66 (9)	1.04−1.17/ 1.09 (9)	1.06−1.13/ 1.09 (9)	$C_{17}/C_{19}/C_{21}$
Chang-7 shale *	0.34−0.57/ 0.46 (15)	0.48−1.15/ 0.72 (15)	0.54−0.84/ 0.72 (15)	1.43−2.33/ 1.81 (15)	1.04−1.08/ 1.06 (15)	1.01−1.08/ 1.04 (15)	$C_{15}/C_{17}/C_{21}$
Chang-8 mudstone *	0.37−0.45/ 0.41 (2)	0.27−0.36/ 0.32 (2)	1.28−1.4/ 1.34 (2)	1.28−1.31/ 1.30 (2)	1.06−1.06/ 1.06 (2)	1.02−1.04/ 1.03 (2)	C_{21}

Notes: * data are cited from Yang et al. (2017), Pr/Ph is pristane/phytane, $\sum nC_{21}^{-}/\sum nC_{21}^{+}$ indicates $(C_{min} + \ldots + C_{21})/(C_{21} + \cdots + C_{max})$, and 0.93/0.75(9) describes max-min/average (sample number). CPI = $\{(C_{25} + C_{27} + C_{29} + C_{31} + C_{33})[1/(C_{24} + C_{26} + C_{28} + C_{30} + C_{32}) + 1/(C_{26} + C_{28} + C_{30} + C_{32} + C_{34})/2\}$, OEP = $[(C_i + 6C_{i+2} + C_{i+4})/4(C_{i+1} + C_{i+3})]^m$, $m = (-1)^{i+1}$, $i + 1$ is the predominant carbon number.

distributed in the "L" type (Yang et al., 2017). The Chang-7 shale and Chang-8 mudstone are characterized by C_{29} sterane predominance and show an inverse "L" distribution (Yang et al., 2017).

4.2 Stable carbon isotope compositions

The carbon isotopes of the total hydrocarbon and crude oil group components are exhibited in Table 4. The $\delta^{13}C_{total\ hydrocarbon}$ values of the Chang-6 mudstone, Chang-7 shale, and Chang-8 mudstone are the heaviest more than −29.1‰, while the $\delta^{13}C_{total\ hydrocarbon}$ values of coal and crude oil samples range from −33.0 ‰ to −29.9‰, and from −32.3‰ to −31.7‰, respectively. The $\delta^{13}C_{total\ hydrocarbon}$ values of three crude oils are lighter than the extract of the source rocks, and between two coal samples (Fig. 4(a)). According to the carbon isotope changes of different components of crude oil samples (Fig. 4(b)), the carbon isotopes of the different components of the An-1 oil and Chang-7 oil present the same characteristics of $\delta^{13}C_{saturated\ hydrocarbon} < \delta^{13}C_{aromatic\ hydrocarbon} < \delta^{13}C_{non\text{-}hydrocarbon} < \delta^{13}C_{asphaltene}$. The $\delta^{13}C$ values of different group components of An-1 oil is lighter than that of Chang-7 oil, implying that the deep-underground crude oil migrated upward and occurred transport fractionation (Curiale and Bromley, 1996). The asphaltene carbon isotope of Chang-8 oil showed abnormal lightening phenomenon and did not become heavier with the increase of polarity. The reason for the abnormal carbon isotopes of Chang-8 oil asphaltene may be due to the increase in burial depth and the strengthening of thermodynamic effects (Saxby and Stephenson, 1987; Price, 1993). Under the action of isotope fractionation, the carbon isotopes of different components increased with increasing polarity. These results were consistent with the funding by Peng et al. (2011).

5 Discussion

5.1 Identification of oil source

To identify the oil sources, the biomarker parameters and carbon isotopes between oil and oil or source rock are often used to evaluate the genetic relationship between them. Since biomarkers are easily affected by microbial degradation, thermal evolution, and geological structure movement, the use of a single biomarker index to identify the oil source is generally insufficient (Liu et al., 2022). Therefore, in this research the source of An-1 oil was determined based on multiple biomarker parameters (Pr/Ph, $Pr/n\text{-}C_{17}$, $Ph/n\text{-}C_{17}$, sterane, terpanes, etc.) and carbon isotopic composition parameter.

According to the redox index of Pr/Ph proposed by Brooks and Smith (1969), the An-1 oil, Chang-7 oil and source rock of Chang-6 and Chang-7 were formed in the reducing environment. Consistently, the correlation diagram between $Pr/n\text{-}C_{17}$ and $Ph/n\text{-}C_{18}$ (Fig. 5(a)) also suggests the existence of crude oil in reducing environment. According to the correlation diagram between $Pr/n\text{-}C_{17}$ and $Ph/n\text{-}C_{18}$ (Shanmugam, 1985), the An-1 oil existing in coal mining face was closely related to Chang-7 oil and Chang-7 source rock. Furthermore, based upon the sedimentary facies identification map developed by Xiao et al. (2018) (Fig. 5(b)), we conclude that the three crude oils were formed in freshwater lake facies, while HL1-5 and HL2-5 coals were formed in marine/salt lake facies and fluvial/deltaic facies, respectively. The correlation diagram of sterane isomerization parameters (Fig. 5(c)) suggest that the An-1 oil, Chang-7 oil, and Chang-8 oil and source rocks were all in the mature stage, indicating that the source rocks had entered the window of oil generation (Xu et al., 2022). According to the triangle diagram of sterane (C_{27}, C_{28}, C_{29}) content (Fig. 5(d)), the parent material input of An-1 oil, Chang-7 oil, and Chang-8 oil is mainly

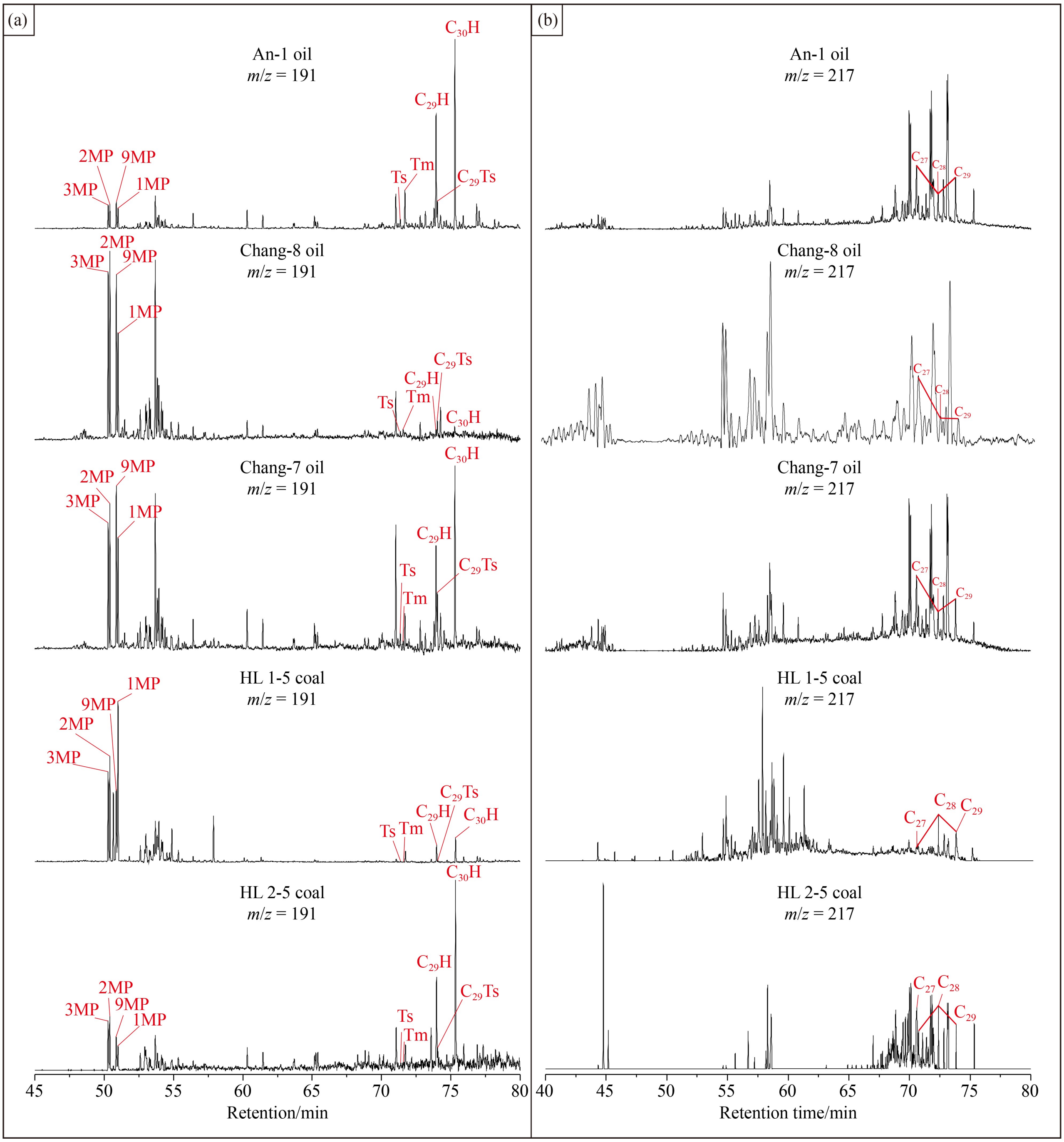

Fig. 3 Chromatogram of steroids and terpenes in crude oil and coal samples.

plankton, while the organic matter of source rock input in Chang-6 and Chang-7 member is mixed. The organic matter of Chang-8 member mainly came from terrestrial plants. The organic matter of HL1-5 and HL2-5 coal samples were generated from the algae and algae predominately. The above analysis of sedimentary facies and parent material type indicate that the An-1 oil cannot generates from the coal seams and source rock of Chang-8 member.

According to the geochemical characteristics of crude oil samples, the main parent material of the An-1 oil, Chang-7 oil, and Chang-8 oil were aquatic organisms (plankton), which were deposited in the reduction environment under the swamp facies, and the crude oils were in the mature stage. Meanwhile, the values of Pr/Ph, Pr/n-C_{17}, Ph/n-C_{17}, sterane, terpanes of An-1 oil were highly similar to those of the Chang-7 oil (Fig. 6). Previous research results show that the carbon isotopic composition of crude oil was controlled by the organic carbon isotopic composition of source rock (Bao et al., 2016) and sedimentary environment (Ogbesejana et al., 2020; Feng et al., 2021), which was an effective method

Table 3 Parameters of steranes and terpenes in crude oils and source rocks

Sample ID	C_{29}20S/(20S+20R)	$C_{29}\beta\beta/(\beta\beta+\alpha\alpha)$	C_{27}/%	C_{28}/%	C_{29}/%	C_{19+20} TT/%	C_{21} TT/%	C_{23} TT/%	*D*
Chang-7 oil	0.82	0.78	43.40	32.30	24.30	34.00	34.30	31.70	L
Chang-8 oil	0.77	0.74	41.30	32.30	26.40	34.10	34.50	31.40	L
An-1 oil	0.85	0.81	43.80	33.00	23.20	34.80	33.80	31.40	L
HL1-5 coal	0.73	0.50	0.40	78.40	21.20	29.00	30.70	40.30	Inverse V
HL2-5 coal	0.76	0.69	12.20	52.50	35.30	52.60	17.90	29.50	Inverse V
Chang-6 mudstone*	0.43−0.50/ 0.45(9)	0.31−0.40/ 0.36(9)	35.50−40.60/ 38.12(9)	30.30−34.10/ 29.5(9)	26.60−33.10/ 29.5(9)	/	/	/	L
Chang-7 shale*	0.43−0.52/ 0.49(15)	0.34−0.4/ 0.37(15)	31.20−39.50/ 32.06(15)	28.40−35.30/ 31.40(15)	27.20−40.80/ 36.56(15)	/	/	/	Inverse L
Chang-8 mudstone*	0.40−0.46/ 0.43(2)	0.37−0.39/ 0.38(2)	15.00−21.20/ 18.10(2)	26.50−30.50/ 28.50(2)	48.40−58.50/ 53.45(2)	/	/	/	Inverse L

Notes: * data are quoted from reference of Yang et al. (2017), 0.43−0.50/0.45(9) is max-min/average (sample number). "/" means the data are missing. *D* is the regular sterane peak shape. $C_{27}\% = C_{27}/(C_{27} + C_{28} + C_{29})$ regular sterane, $C_{28}\% = C_{28}/(C_{27} + C_{28} + C_{29})$, $C_{29}\% = C_{29}/(C_{27} + C_{28} + C_{29})$, $C_{19+20}TT\% = C_{19+20}TT/(C_{19+20}TT + C_{21}TT + C_{23}TT)$, $C_{21}TT\%$ = C21TT/($C_{19+20}TT + C_{21}TT + C_{23}TT$), $C_{23}TT\% = C_{23}TT/(C_{19+20}TT + C_{21}TT + C_{23}TT)$.

Table 4 Carbon isotopes of the total hydrocarbon and crude oil's group components

Sample ID	$\delta^{13}C_{total\ hydrocarbon}$/(‰, PDB)	$\delta^{13}C_{group\ components}$/(‰, PDB)			
		Saturated hydrocarbon	Aromatic hydrocarbon	Nonhydrocarbon	Asphaltene
Chang-7 oil	− 31.7	− 32.0	− 30.0	− 28.9	− 27.3
Chang-8 oil	− 32.3	− 32.6	− 30.8	− 29.5	− 31.5
An-1 oil	− 31.8	− 32.3	− 31.1	− 29.8	− 27.5
HL1-5 coal	− 29.9	/	/	/	/
HL2-5 coal	− 33.0	/	/	/	/
Chang-6 mudstone*	− 26.9− − 30.0/−28.9 (9)	/	/	/	/
Chang-7 shale*	− 28.60− − 29.8/−29.0 (15)	/	/	/	/
Chang-8 mudstone*	− 28.2− − 30.0/−29.1 (2)	/	/	/	/

Notes: * data are cited from Yang et al. (2017), "/" means no test, and − 26.9− − 30.0/−28.93(9) describes max-min/average (sample number).

for oil source correlation (Stahl, 1978). It is generally believed that carbon isotope deviations within ± 1 ‰ can be considered homologous (Fuex, 1977). According to the carbon isotope curve of crude oil group components (Fig. 4(b)), the carbon isotope curve of An-1 oil and Chang-7 oil maintains a good correlation, and the average difference of carbon isotopes of different group components was approximately 0.6 ‰. Therefore, the distribution of carbon homologs of different group components of An-1 oil and Chang-7 oil was in good consistency. We infer that the An-1 oil is generated from the source rocks of Chang-7 member or/and Chang-6 member, but not Chang-8 member.

5.2 Accumulation mode of An-1 oil occurring in the coal seam

The Huangling mining area, located on the southern margin of the Ordos Basin, suffered from serious tectonic activity during Mesozoic and developed deformation with many joints and fractures. These joints and fractures improve the reservoir porosity and permeability and migration channels of oil (Li et al., 2019b). Based on the correlation of oil-oil and oil-source rock, a migration and accumulation model of An-1 oil in the Huangling mining area is proposed (Fig. 7). The Chang-6 and Chang-7 members of the Yanchang Formation are excellent source rocks in this area. After entering into the oil-generating window, the source rocks of Chang-6 and Chang-7 members begin to generate crude oil. The Chang-7 oil was generated from the Chang-7 source rock or from both Chang-6 and Chang-7 source rocks and then accumulated in the Chang-7 member. The Chang-7 oil migrates upward along the fissure, which is driven by high pressure. The simulation results of tectonic evolution showed that the fissure was opened since the stratum was uplifted in the early of Later Cretaceous (Bao et al., 2021b). Therefore, the An-1 oil is generated from the Yanchang Formation (Chang-6 and Chang-7 source rocks) and occurred in the coal seam during the stratum uplift stage of Himalayan tectonic period.

6 Conclusions

The source and accumulation model of An-1 oil occurring

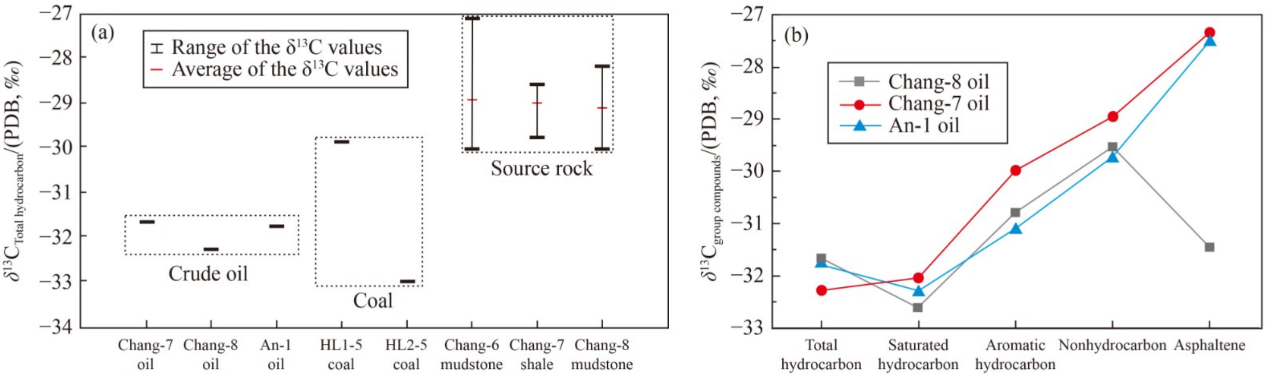

Fig. 4 Relationship of carbon isotopic compositions in coal and oil samples. (a) Carbon isotopes of total hydrocarbon; (b) carbon isotopes of group components.

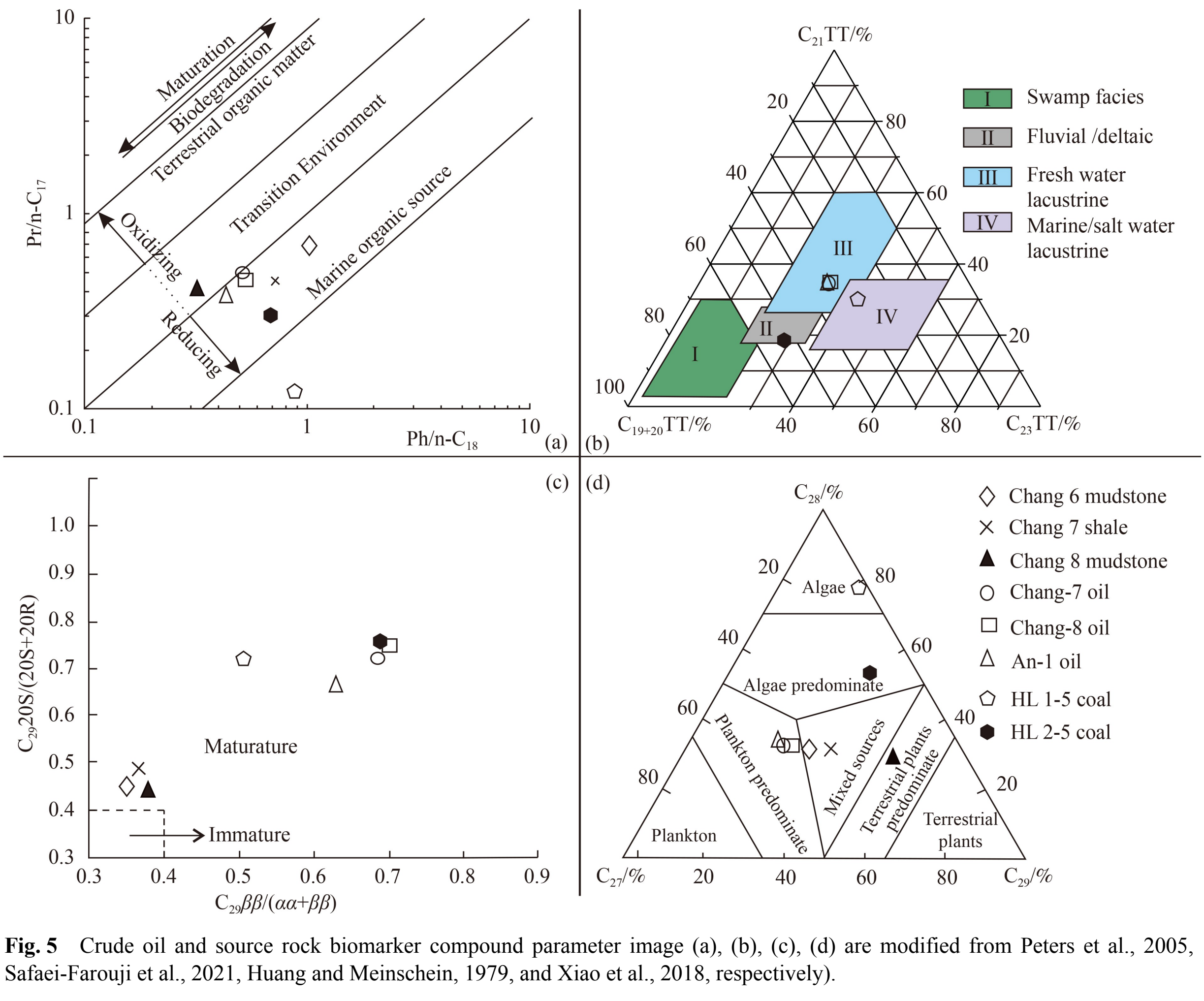

Fig. 5 Crude oil and source rock biomarker compound parameter image (a), (b), (c), (d) are modified from Peters et al., 2005, Safaei-Farouji et al., 2021, Huang and Meinschein, 1979, and Xiao et al., 2018, respectively).

in the Jurassic No. 2 coal seam were investigated based on the biomarker components analysis and stable isotope ratio using mass spectrometry and gas chromatography–mass spectrometry tests. The main conclusions are as follows.

1) Based on the identification of crude oil with multiple biomarker compound parameters, the source input of An-1 oil is mainly aquatic organisms (plankton), which are deposited in a reducing environment, and the sedimentary facies is freshwater lake facies.

2) The An-1 oil has the similar geochemical characteristics with the Chang-7 oil based on the biomarker analysis and oil source correlation.

3) The correlation of oil-source rock indicate that the An-1 oil was generated from Chang 7 member or from both Chang-7 and Change 6 members while Chang-8 and

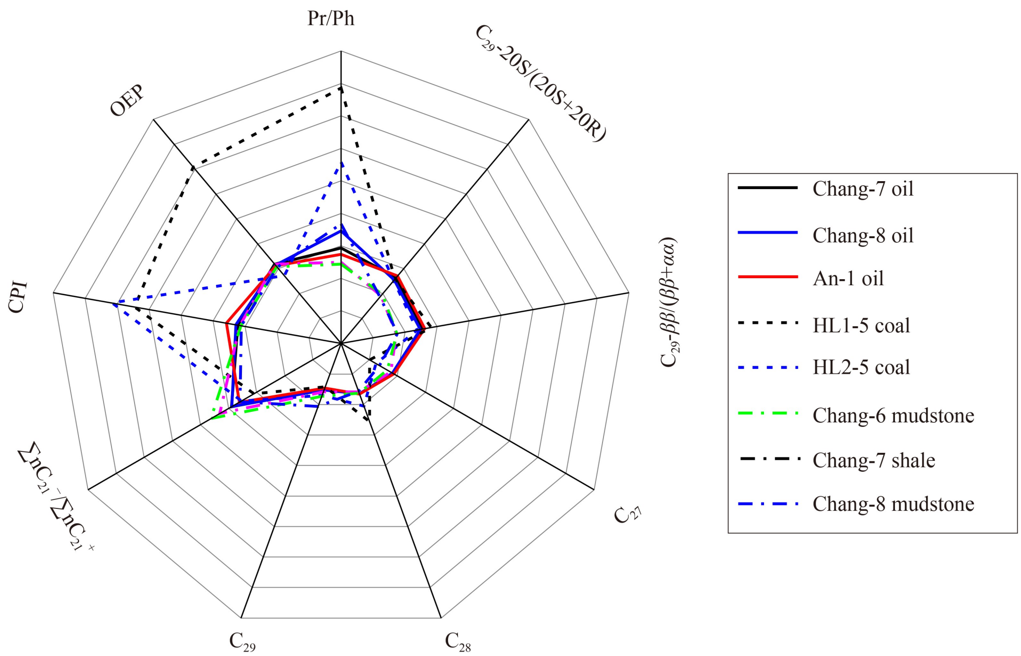

Fig. 6 The star chart of biomarker parameters.

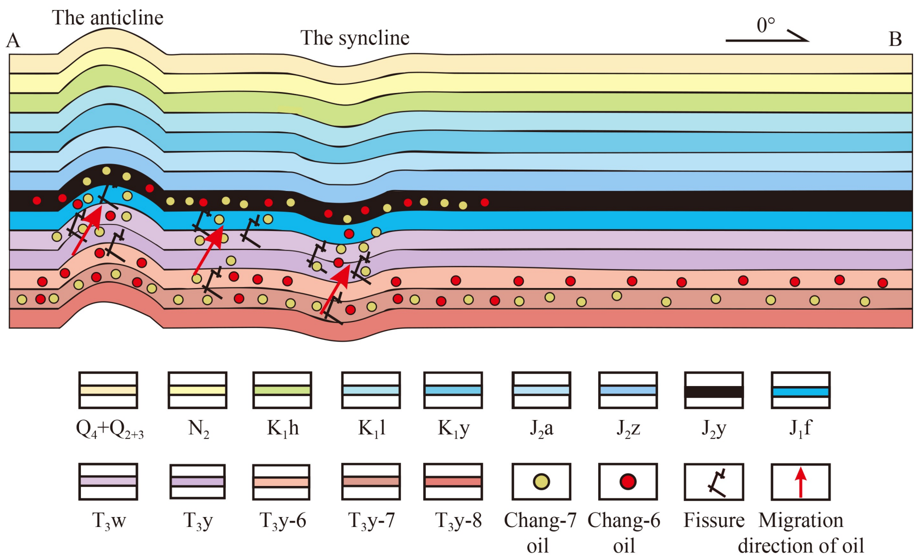

Fig. 7 Schematic diagram of An-1 oil's migration and occurrence in the Huangling mining area.

coal were not its source rocks. During the period of Himalayan orogeny, the Chang-7 oil migrated upward along the fissure and accumulated in the Jurassic No. 2 coal seam.

Acknowledgments This work was supported by the National Natural Science Foundation of China (Grant Nos. 42172200 and 41972183); and the "Chunhui Plan" Cooperative Research for Ministry of Education.

References

Abdullah E S, Ebiad M A, Rashad A M, Nady M M, El-Sabbagh S M (2021). Thermal maturity assessment of some Egyptian crude oils as implication from naphthalene, phenanthrene and alkyl substituents. Egypt J Pet, 30: 17–24

Bao J, Chen X, Zhu C (2016). Novel ^{15}C sesquiterpene and its source origin in the crude oil of the Pearl River Mouth Basin. Sci China Earth Sci, 59(8): 1622–1632

Bao Y, Li D, Ju Y (2021a). Constraints of biomethane generation yield and carbon isotope fractionation effect in the pathway of acetotrophic with different coal-rank coals. Fuel, 305: 121493

Bao Y, Tang J, Ju Y, An C (2021b). Tectonic-thermal evolution and biogas generation of source rocks from the mesozoic coal measures at the Huangling mining area, southeastern margin of Ordos Basin. Adv Earth Sci, 36(10): 993–1003 (in Chinese)

Bao Y, Wang W, Ma D, Shi Q, Ali A, Lv D, Zhang C (2020). Gas origin and constraint of $\delta^{13}C(CH_4)$ distribution in the Dafosi mine field in the southern margin of the Ordos Basin, China. Energy Fuels, 34(11): 14065–14073

Brooks J D, Smith J W (1969). The diagenesis of plant lipids during the formation of coal, petroleum and natural gas—II. coalification and the formation of oil and gas in the Gippsland Basin. Geochim Cosmochim Acta, 33(10): 1183–1194

Chen D D (2018). Multi-factor coupling regional prediction technology of surrounding rock gas in coal and gas symbiotic mine: a case study of Huangling mining area in Ordos Basin. Coal Geol Explor, 46(02): 49–53 (in Chinese)

Curiale J A, Bromley B W (1996). Migration induced compositional changes in oils and condensates of a single field. Org Geochem, 24(12): 1097–1113

Deng J, Wang Q, Gao B (2005). Evolution of Ordos Basin and its distribution of various energy and mineral resources. Geosci, 19(4): 538–545 (in Chinese)

Feng D, Pohlman J W, Peckmann J, Sun Y, Hu Y, Roberts H H, Chen D (2021). Contribution of deep-sourced carbon from hydrocarbon seeps to sedimentary organic carbon: evidence from radiocarbon and stable isotope geochemistry. Chem Geol, 585: 120572

Fu J, Zhang Z, Chen C, Wang T, Li M, Ali S, Lu X, Dai J (2019). Geochemistry and origins of petroleum in the Neogene reservoirs of the Baiyun Sag, Pearl River Mouth Basin. Mar Pet Geol, 107: 127–141

Fuex A N (1977). The use of stable carbon isotopes in hydrocarbon exploration. J Geochem Explor, 7(77): 155–188

Huang F, He L, Wu Q (2015). Lithospheric thermal structure of the Ordos Basin and its implications to destruction of the North China Craton. Chin J Geophys, 58: 3671–3686

Huang W, Meinschein W G (1979). Sterols as ecological indicators. Geochim Cosmochim Acta, 43(5): 739–745

Huang Z, Sednek C, Urynowicz M A, Guo H, Wang Q, Fallgren P, Jin S, Jin Y, Igwe U, Li S (2017). Low carbon renewable natural gas production from coalbeds and implications for carbon capture and storage. Nat Commun, 8(1): 568

Hunt J M (1991). Generation of gas and oil from coal and other terrestrial organic matter. Org Geochem, 17(6): 673–680

Ji L, He C, Zhang M, Wu Y, Li X (2016). Bicyclic alkanes in source rocks of the Triassic Yanchang Formation in the Ordos Basin and their inconsistency in oil-source correlation. Mar Pet Geol, 72: 359–373

Jiang Y, Bhattacharyya D (2016). Process modeling of direct coal-biomass to liquids (CBTL) plants with shale gas utilization and CO_2 capture and storage (CCS). Appl Energy, 183: 1616–1632

Kotarba M J (2012). Origin of natural gases in the Paleozoic-Mesozoic basement of the Polish Carpathian Foredeep. Geol Carpath, 63(4): 307–318

Li D, Bao Y, Wang Y, An C, Chang J (2023). Multiple-experimental investigation on the physicochemical structures alternation during coal biogasification. Fuel, 339: 127433

Li S, Ma Y, Yu X, Li A (2017b). Reservoir potential of deep-water lacustrine delta-front sandstones in the upper Triassic Yanchang formation, Western Ordos Basin, China. J Pet Geol, 40(1): 105–118

Li Y, Pan S, Ning S, Shao L, Jing Z, Wang Z (2022). Coal measure metallogeny: metallogenic system and implication for resource and environment. Sci China Earth Sci, 65(7): 1211–1228

Li Y, Wang Z, Gan Q, Niu X, Xu W (2019b). Paleoenvironmental conditions and organic matter accumulation in Upper Paleozoic organic-rich rocks in the east margin of the Ordos Basin, China. Fuel, 252: 172–187

Li Y, Yang J, Pan Z, Meng S, Wang K, Niu X (2019a). Unconventional natural gas accumulations in stacked deposits: a discussion of Upper Paleozoic coal-bearing strata in the east margin of the Ordos Basin, China. Acta Geol Sin Engl Ed, 93(1): 111–129

Li Y, Zhang C, Tang D, Gan Q, Niu X, Wang K, Shen R (2017a). Coal pore size distributions controlled by the coalification process: an experimental study of coals from the Junggar, Ordos, and Qinshui basins in China. Fuel, 206: 352–363

Liu W, Liao Y, Jiang C, Pan Y, Huang Y, Wang X, Wang Y, Peng P (2022). Superimposed secondary alteration of oil reservoirs. Part II: the characteristics of biomarkers under the superimposed influences of biodegradation and thermal alteration. Fuel, 307: 121721

Liu X, Wang F, Liu B, Tian J, Shang T, Ma J, Zhang Z, Zhang X (2020). Factors controlling hydrocarbon accumulation in Jurassic reservoirs in the southwest Ordos Basin, NW China. Acta Geol Sin Engl Ed, 94: 467–484

Ogbesejana A B, Bello O M, Ali T (2020). Origin and depositional environments of source rocks and crude oils from Niger Delta Basin: carbon isotopic evidence. China Geol, 3: 602–610

Peng J, Liu G, Luo K, Lv J (2011). Comparison of oil source and analysis of hydrocarbon accumulation history in Kaili area. J Southwest Petrol Univ (Nat Sci Ed), 33(3): 61–66+193 (in Chinese)

Peters K E, Walters C C, Moldowan J M (2005). The Biomarker Guide: Biomarkers and Isotopes in Petroleum Systems and Earth History. UK: Cambridge University Press

Price L C (1993). Thermal stability of hydrocarbon in nature: limits evidence characteristics and possible controls. Geochim Cosmochim Acta, 57(14): 3261–3280

Safaei-Farouji M, Kamali M R, Rahimpour-Bonab H, Gentzis T, Liu B, Ostadhassan M (2021). Organic geochemistry, oil-source rock, and oil-oil correlation study in a major oilfield in the Middle East. J Petrol Sci Eng, 207: 109074

Saxby J D, Stephenson L C (1987). Effect of an igneous intrusion on oil shale at Rundle (Australia). Chem Geol, 63(1–2): 1–16

Shanmugam G (1985). Significance of coniferous rain forests and related organic matter in generating commercial quantities of oil, Gippsland Basin, Australia. AAPG Bull, 69: 1241–1254

Stahl W J (1978). Source rock-crude oil correlation by isotopic type-curves. Geochim Cosmochim Acta, 42(10): 1573–1577

Su X, Zhao W, Xia D, Hou S, Fu H, Zhou Y (2022). Experimental study of advantages of coalbed gas bioengineering. J Nat Gas Sci Eng, 102: 104585

Volkman J K, Farrington J W, Gagosian R B, Wakeham S G (1983). Lipid composition of coastal marine sediments from the Peru upwelling Region. Adv Org Geochem, 1981: 228–240

Wang Q, Hao F, Xu C, Zou H (2020). Paleolimnological environments and the formation of high quality source rocks in the Bohai Bay Basin: an integrated geochemical study of biomarkers, stable carbon and oxygen isotopes, and trace elements. J Petrol Sci Eng, 195:

107753

Ward C R (2002). Analysis and significance of mineral matter in coal seams. Int J Coal Geol, 50(1–4): 135–168

Whiticar M J (1996). Stable isotope geochemistry of coals, humic kerogens and related natural gases. Int J Coal Geol, 32(1–4): 191–215

Xiao H, Wang T, Li M, Fu J, Tang Y, Shi S, Yang Z, Lu X (2018). Occurrence and distribution of unusual tricyclic and tetracyclic terpanes and their geochemical significance in some Paleogene oils from China. Energy Fuels, 32(7): 7393–7403

Xu M, Hou D, Lin X, Liu J, Ding W, Xie R (2022). Organic geochemical signatures of source rocks and oil-source correlation in the Papuan Basin, Papua New Guinea. J Petrol Sci Eng, 210: 109972

Yang Y, Zhou S, Li J, Li C, Li Y, Ma Y, Chen K (2017). Geochemical characteristics and oil-source correlation of source rocks in Yanchang Formation, southern margin of Ordos Basin. Nat Gas Geosci, 28(4): 550–565 (in Chinese)

Yi L, Liu Z, Chen Z, Li M (2020). Thermal maturity, source characteristics, and migration directions for the Ordovician oil in the Central Tabei Uplift, Tarim Basin: insight from biomarker geochemistry. J Petrol Sci Eng, 189: 106975

Zhang M, Liu C, Tian J, Lu Z, Pang H, Zeng X, Kong H, Yang S (2020). Geochemical characteristics of crude oil and oil-source correlation in the western Qaidam Basin, China. Nat Gas Geosci, 31(1): 61–72 (in Chinese)

Zhang X, Shen B, Yang J, Sun W, Hou D (2021). Evolution characteristics of maturity-related sterane and terpane biomarker parameters during hydrothermal experiments in a semi-open system under geological constraint. J Petrol Sci Eng, 201: 108412

Zhao Y, Yao J, Sun B, Yi D, Dong C, Deng X, Liu L (2014). Evidence of oil sources and migration in Triassic-Jurassic reservoirs in the South Tianhuan depression of the Ordos Basin, China based on analysis of biomarkers and nitrogen-bearing compounds. Acta Geol Sin Engl Ed, 88(6): 1798–1810